ORIGINAL RESEARCH PAPER

Temperature Measurement and Distribution Inside Planar SOFC Stacks

W. B. Guan[1], H. J. Zhai[1], L. Jin[1], C. Xu[1], and W. G. Wang[1]*

[1] Ningbo Institute of Material Technology and Engineering (NIMTE), Chinese Academy of Sciences, Ningbo 315201, PR China

Abstract

In this work, a kind of thin K-type thermocouple and self-developed CAS-I sealant were used to assembly solid oxide fuel cell (SOFC) stacks and temperatures of unit cells inside a planar SOFC stack were measured. The open circuit voltage testing of the stack and characterization of the interface between sealant and components suggested excellent sealing effect by applying the developed method. The effect of discharging direct-current on temperature and temperature distribution inside the designed SOFC stack was investigated. The results showed that the discharging current had a great impact and the gas flow rate had a slight impact on the temperatures of unit cells. Temperature distribution of unit cells inside the stack was much non-uniform and there is a significant temperature difference between various components of the stack and heating environment. The relationship between temperatures and cell performance showed that the worse the cell performance, the higher the cell surface temperature. When the stack was discharged at a constant current and the temperature of cell surface was over 950 °C, the higher the temperature, the more drop the corresponding voltage.

Keywords: Sealant, Solid Oxide Fuel Cells, Stack, Temperature Distribution, Temperature Measurement

1 Introduction

Temperature distribution is an important parameter to determine performance of single cells and stacks for solid oxide fuel cells (SOFC) [1–3], and is also a key issue to induce thermal stress of various components within SOFC stacks [4–7]. A core issue of stack design is to obtain uniform temperature distribution and minimize thermal stress between components resulting from temperature difference. Therefore, it is important to know temperature gradient and distribution for stack design and performance analysis. Up to now, theoretical simulation was used to predict temperature gradient and distribution in stacks [8,9], but in most cases, it can not accurately predict temperature gradient and distribution, and not allow us to truly understand them. So, it is necessary to *in-situ* measure temperature in stacks by experimental methods.

Planar SOFC stacks are composed of metal interconnects, sealing materials, and unit cells [10,11]. High performance of SOFC stacks requires that the space between metal interconnects and unit cells is small and the stack is gastight, which causes the problem for inserting thermocouples into stacks.

To successfully measure the temperatures inside stacks, the thermocouples must be thin and the sealing materials can work properly in the presence of thermocouples. Due to the above problems, there is no literature report of experimental testing result about temperature measurement inside stacks.

This work aims to develop an experimental method to measure temperatures inside stacks under operating temperatures and experimental environment, and uses this method to obtain the temperature gradient inside a three-unit cell stack. The impact of parameters such as gas flow rates, direct-current (DC) discharging, and discharging time on the temperatures of cell surfaces within the stack were investigated. The result shows that the chosen sealant has an excellent sealing effect, and the discharging DC has a significant effect and the gas flow rate has a slight effect on the temperatures. Moreover, the temperature distribution inside the stack is much non-uniform, and the appearance of high temperatures is a sign of the decay of unit cell inside the stack.

---

[*] *Corresponding author, wgwang@nimte.ac.cn*

2 Experimental Procedures

2.1 Stack Design and Temperature Measurement Methods

A three-unit cell stack was assembled, and thermocouple probes and voltage probes were arranged according to the schematic diagram, as shown in Figure 1. SUS430 ferritic stainless steel was applied to make metal interconnects, which is also used as co-flow gas channels in this work. The gas flow channels of the interconnect were etched with size of 10 mm × 1.5 mm, of which the height of channel tip was about 0.6 mm. In the stack, the porous nickel was put on the anode side of interconnect as anode current collecting layer. To protect the high temperature oxidation and Cr vaporization, the cathode side of interconnect was coated densely with $(La_{0.75}Sr_{0.25})_{0.95}MnO_3$ (LSM) micro-spherical powders by plasma spray technology. The three anode-supported unit cells with composition of Ni-YSZ/YSZ/LSM were used to assembly the stack. The unit cells were produced by Ningbo Institute of Material Technology & Engineering (NIMTE). The active area of unit cell is 10 cm × 10 cm with total area of 13 × 13 cm^2, and the other parameters were reported by the previous publication of our group [12]. The contact area between the interconnect and the cell electrode is about 25% of the cell active area. A kind of SiO_2-Al_2O_3-based ceramic sealant (CAS-I) was used as sealing materials between metal interconnects and unit cells. In this
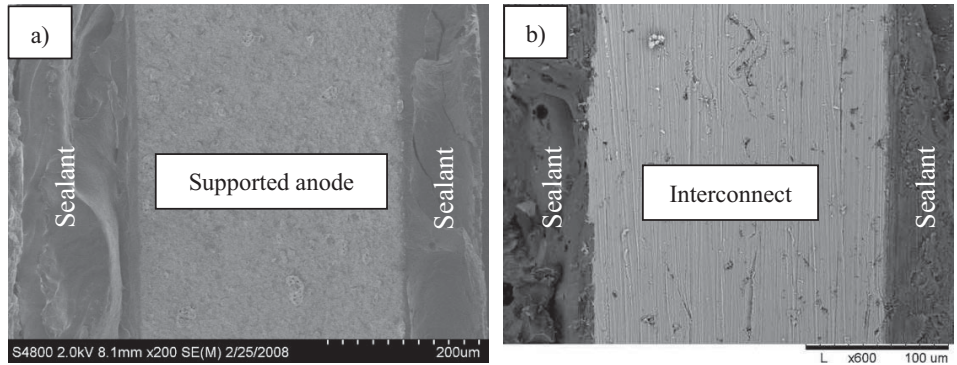

Fig. 2 (a) Morphology of interface between sealants and unit cells; (b) morphology of the interface between sealants and interconnects.

work, when a thermocouple was inserted into the stack to measure the temperature, gas leakage of the stack will happen generally. In order to avoid the phenomenon being appeared, the thermocouple needs being inserted from the middle of sealant. To accomplish this work, two pieces of sealant were assembled together, which is named multi-layer sealant in this work. After the stack being assembled, the hydrogen (H_2) was fed into the stack anode channel through the fuel inlet pipe. The NiO-YSZ supported anode was reduced by H_2 at a given temperature for about 5 hours. Thereafter, the air was fed into the stack cathode channel through the oxidizing gas pipe. The flow direction of fuel and air in stack can be seen in Figure 1. After testing, the morphology of interface between sealants and components of stack was shown in Figure 2. The sealant was combined with interconnect and supported anode of unit cell tightly, indicating excellent sealing effect. As can be seen from Figure 2, the thickness of sealant is generally less than about 100 μm after sintering.

The thermocouple used in this work was a thin K-type thermocouple (as seen in Figure 3), and can measure the maximum measurement temperature of 1200 °C. The anode of the thermocouple was made by nominal composition of $Ni_{90}Cr_{10}$ and the negative was made by $Ni_{97}Si_3$, respectively. This kind of K-type thermocouple can be used in temperature measurement inside stack operating environments due to its
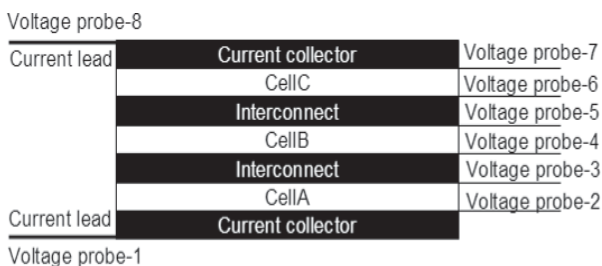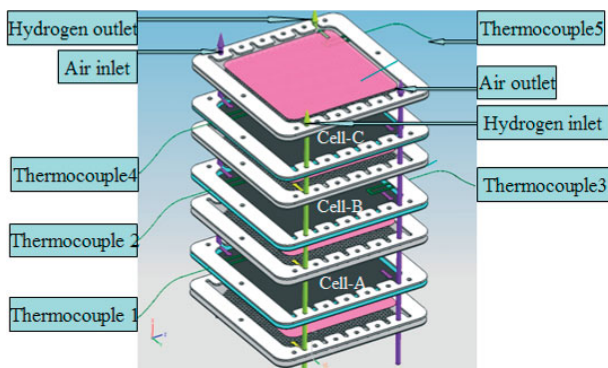

Fig. 1 Schematic diagram of gas flow, thermocouple probe (top), and voltage probe locations (bottom) inside a three-unit cell stack.
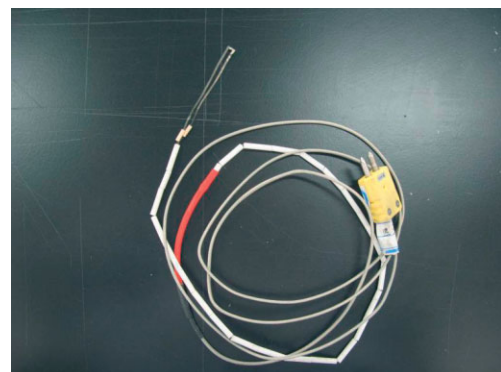

Fig. 3 The thin-K type thermocouple.

high sensitivity, stability, homogeneity, and high temperature oxidation resistance. To measure the temperature inside the stack during operation, the thermocouple should be inserted into the stack. The gas would normally leak from the position where the thermocouple inserted. Therefore, the multi-layer sealant was applied as mentioned above. While the space of the sealant after sintering is small. The thermocouples also have to be thin and small, and preferably less than 100 μm thickness. Then, the thermocouple was manufactured to be about 10 μm thickness. The measuring point of thermocouple probes was pasted on the surface of interconnect. The heat conduction in gases is much poor, and needs about more than 100 min to make the temperature maintaining stable after gases being fed into the stack in the absence of the discharge state. While in the state of discharge, the heat produced by discharge current inside stack will be transferred to metal interconnect and thermocouple first due to their high thermal conductivity comparison with that of gases in stack. Therefore, the increased temperature induced by discharge current should be measured by the K-type thin thermocouple in a short time. The outside part of the thermocouple was put inside Al_2O_3 tube in order to prevent short-circuit from contact between thermocouples and outside surfaces of the stack. As shown in Figure 1, thermocouple 1, 2, and 4 were located at the air entrances (position 1, 2, 4) of cell A, B, C, respectively. Thermocouple 3 (position 3) was located at the air outlet of cell B, and thermocouple 5 (position 5) was located at the total hydrogen outlet.

To investigate the relationship between temperatures and cell performance, high purity nickel wires with the thickness of about 0.01 mm were used as voltage probes and were put on both electrode sides of cells. The nickel wire probes were made from the nickel wires of 1.0 mm thickness pressed under high pressure using rolling machine, and located in the middle of multi-layer sealing materials as indicated in Figure 1. The outside part of nickel wire was inserted into Al_2O_3 tube to prevent contacting with the stack and the thermocouples.

2.2 Characterization and Stack Operation

In order to investigate the performance of the sealing material under stack operation and thermal cycling, the CAS-I sealing material was suppressed into a small cylinder with size of $\Phi 8.5 \times 5$ mm, and then the sealing material cylinder was placed in the SJY-type high-temperature sintering imaging instrument with a heating rate of 1 °C min^{-1} from
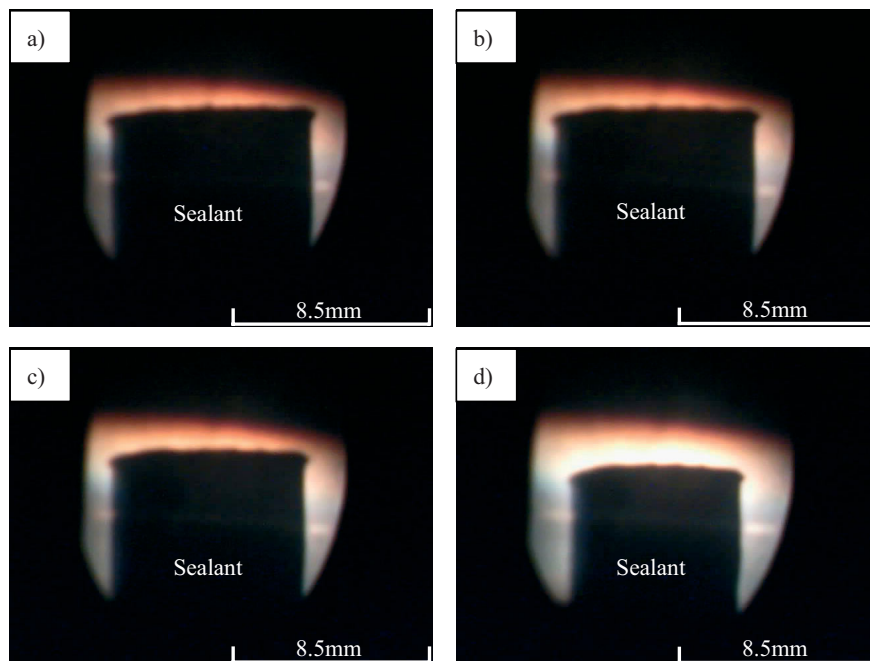

Fig. 4 Morphology of sealing glass at different temperatures: (a) 200 °C, (b) 750 °C, (c) 800 °C, (d) 850 °C.
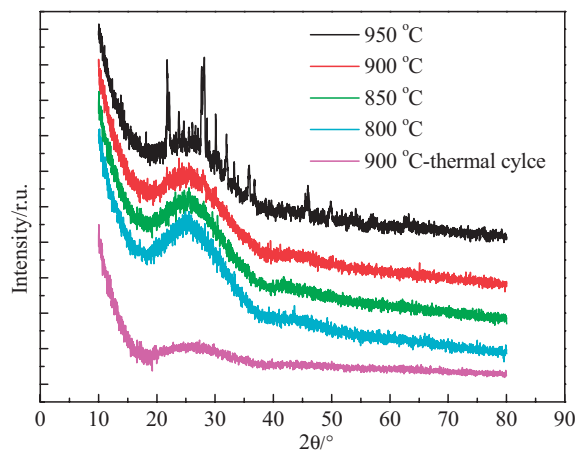

Fig. 5 XRD patterns of sealing glass before and after thermal cycle at different temperature.

room temperature to 900 °C. The high temperature deformation process was recorded, as represented in Figure 4. The crystal structure was investigated by D8 Advance XRD, as shown in Figure 5. Also, the sealant was applied in unit stack, and thermal cycling experiments were carried out to verify the sealing performance by measuring the stack open circuit voltage (OCV), as indicated in Figure 6. The element distribution in interface between sealants and SOFC components was investigated by SEM spectroscopy with EDS attachment, as seen in Figure 7.

The assembled stack was put into the furnace with maximum temperature of 1,200 °C and heated by the rate of 1 °C min^{-1} to 850 °C, and then the temperature was maintained at 850 °C. N$_2$ gas was used to purge and protect the
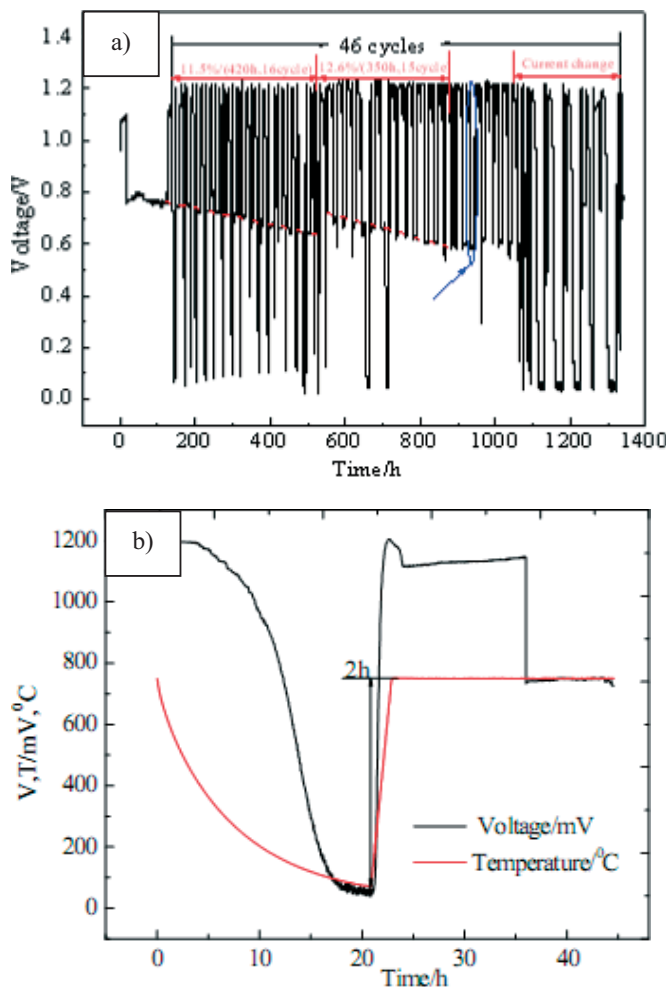
Fig. 6 The OCV tests of one-cell stack and thermal cycling process.

stack being oxidized during the heating process. After keeping the stack at the temperature of 850 °C for more than 60 min, a certain amount of external pressure was loaded on the stack in order to ensure an excellent sealing effect at high temperatures, and then hydrogen and air were fed into the anode and cathode of stack, respectively. After reduction by H_2 at 850 °C for about 5 h, the experiment of temperature measurement under various conditions was carried out. The results of electrochemical measurements and temperature measurements were shown from Figures 8–12.

3 Experimental Results and Discussions

The performance of the sealant is a key factor to impact on sealing effect and thermal cycling performance of SOFC stack during temperature measurement. Therefore, it is necessary to investigate its deformation and crystal structure before and after thermal cycling. The thermal cycling process can be divided into two stages in this work. The first stage involves the process of heating from 50 °C to 900 °C with rate of 5 °C min^{-1} and then holding at 900 °C for over 5 h. The sec-

ond stage involves the process of cooling from 900 °C to 50 °C with rate of 5 °C min^{-1}. The length of the thermal cycle is about 640 min. It can be seen from Figure 4 that the size of sealing material began to change at the temperature of about 800 °C, and changed greatly at about 850 °C, indicating that the sealant has signs of softening at about 800 °C and softened obviously after 850 °C. The XRD patterns of the sealing materials at different temperatures from 800 °C to 950 °C and after thermal cycling condition mentioned above were shown in Figure 5. It was found that the sealing materials are amorphous and no obvious phase change before and after thermal cycling below 900 °C. While some crystallization peak appeared in the XRD patterns of the sealant at the temperature of 950 °C. The results indicated that the sealant has a proper sealing and thermal cycling performance below the temperature of 900 °C. To verify the CAS-I sealant sealing and thermal properties in SOFCs, a one-cell stack was assembled according to the stack design in this work, and the OCV was measured under thermal conditions, as seen in Figure 6a. In the stack, the thermal cycling process can be seen in Figure 6b, in which the time of each thermal cycle is about 50 h from room temperature to 750 °C. It can be seen that the OCV of the stack always remains more than 1.1 V and keeps stable under 46 thermal cycles. Apparently, the self-developed CAS-I sealant is suitable for use in stack sealing and has a proper thermal cycling performance. The element distribution at the interface between sealants and components (containing Ni-YSZ/YSZ half cell and SUS430 stainless steel interconnect, respectively) after sintering at 850 °C was shown in Figure 7. It can be seen clearly that the main elements Si, O, Ca Al of sealants and the main elements Zr and Ni of half cells did not diffuse into each other. Figure 7 also showed that the elemental distribution of the interface between sealants and interconnects. The result indicated that the main elements of Al, O, Ca, and Si of sealant and the main elements of Cr and Fe of the interconnect did not diffuse at the interface, either. The results suggested that the sealant has a proper chemical stability at the interface between sealants and components for SOFC stacks. The images of sealant at different temperatures and elemental distribution of interface indicated that CAS-I can work properly below 900 °C. To further verify the sealing effect of the stack with the thin K-type thermocouple installing inside the stack, the OCV of assembled stack was tested under various conditions. The initial OCV of the three-cell stack and unit cell was up to 3.3 V and 1.1 V, respectively, and remained more than 3.3 V and 1.1 V after two thermal cycles and operation time of 150 h, which indicated a good sealing effect by using CAS-I sealing materials, even under the conditions that the K-type thermocouple was inserted into the stack from the middle of the multi-layer sealant. Although the temperatures of the unit cell surface can reach 1,000 °C (discuss later in this paper), the margins of the SOFC stack operated at 850 °C is around 850 °C, which is in the range of working temperatures of CAS-I sealing materials.
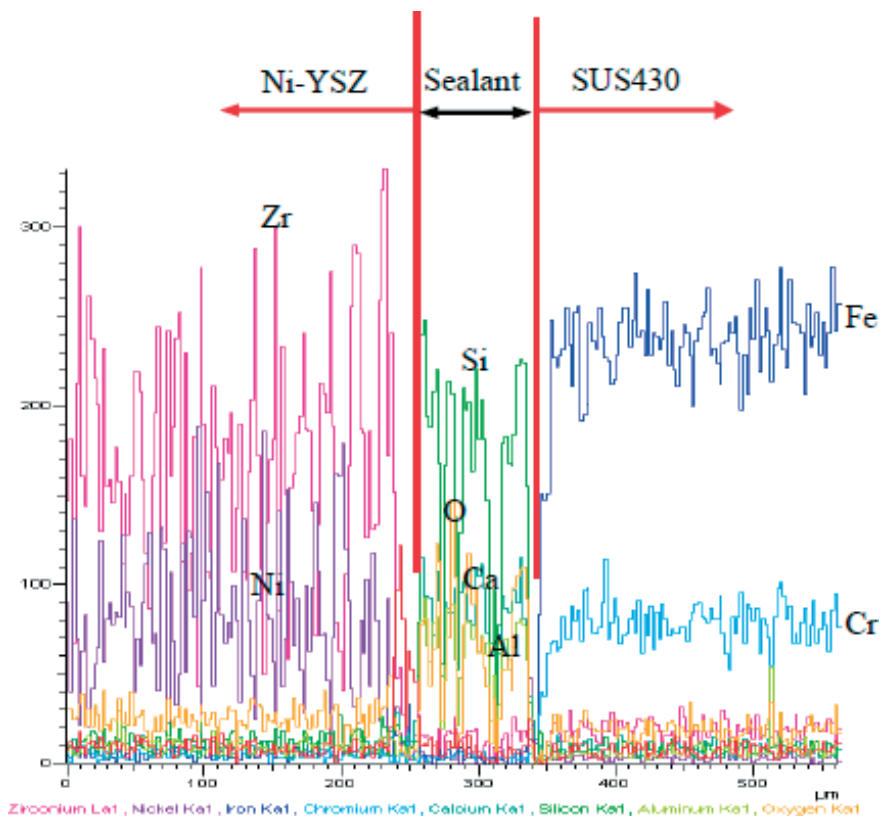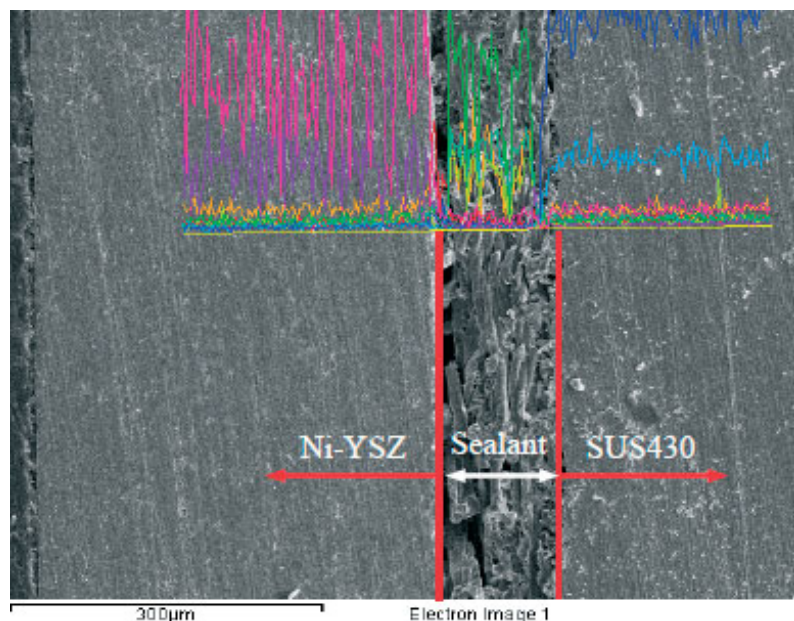
Fig. 7 EDS line scan of the interface of (half cell) Ni-YSZ/Sealant/SUS430 (interconnect).

temperatures in the stack were achieved in 150 min. Moreover, the temperatures within the stack increased following the order of the position 1, 2, 4, 5–3. The above order is reasonable since position 3 with the highest temperature was located on the air exit of cell B, and position 1 with the lowest temperature was located on the air entrance of cell A. After 275 min of running time, the maximum temperature and the minimum temperature inside the stack were 833 °C and 792 °C, which shows the temperature differences of 17 °C and 58 °C with the heating oven temperature of 850 °C, respectively. The temperature of air inlet position 1,2,4, on the surface of cell A, B, C within stack were 792 °C, 800 °C, 813 °C, respectively. The temperature difference between air inlet position 2 and outlet position 3 of cell B was about 20 °C, which is due to gas continuously being heated in the path from import position 2 to export position 3.

The influence of DC (exothermic reaction) on temperatures within the stack under various gas flow rates was shown in Figure 8b. To exclude the influence of operation time on temperatures inside the stack, each condition was maintained for a short time. If the time stays too long, the heat produced by current will be transferred to gases and blown away by gases. The effect of current on temperature change will be covered by gas heat transfer. It was found that holding for 10 s is much appropriate for recording the data during experiments. Comparison of temperatures of each position under the same current in Figure 8b, it was suggested that the effect of gas flow rates on temperatures inside the stack is small under a low constant current within a short time, and the temperatures of various parts of the stack except position 5 linearly increased with the current increasing under a constant gas flow rate. Since the exothermic reaction has taken place in cathode side, the temperature at position 5, the total hydrogen outlet of the stack, remained relatively constant. When the current reaches 5 A, the temperature at air outlet position 3 of cell B is around 1,000 °C, and the maximum temperature difference inside the stack is more than 200 °C, regardless of gas flow rates. Therefore, it can be seen clearly that the current had a significant impact on the temperatures within the stack. Figure 9 shows the *I–V*

The assembled stack was operated at 850 °C according to the procedures described in experimental sections. The change of temperatures with time course for various locations within the three-cell stack without discharging currents (no exothermic reaction) was shown in Figure 8a. The result shows that, under the condition of 3.33 sccm cm^{-2} (cell surface) of hydrogen and 6.67 sccm cm^{-2} of air, relatively stable
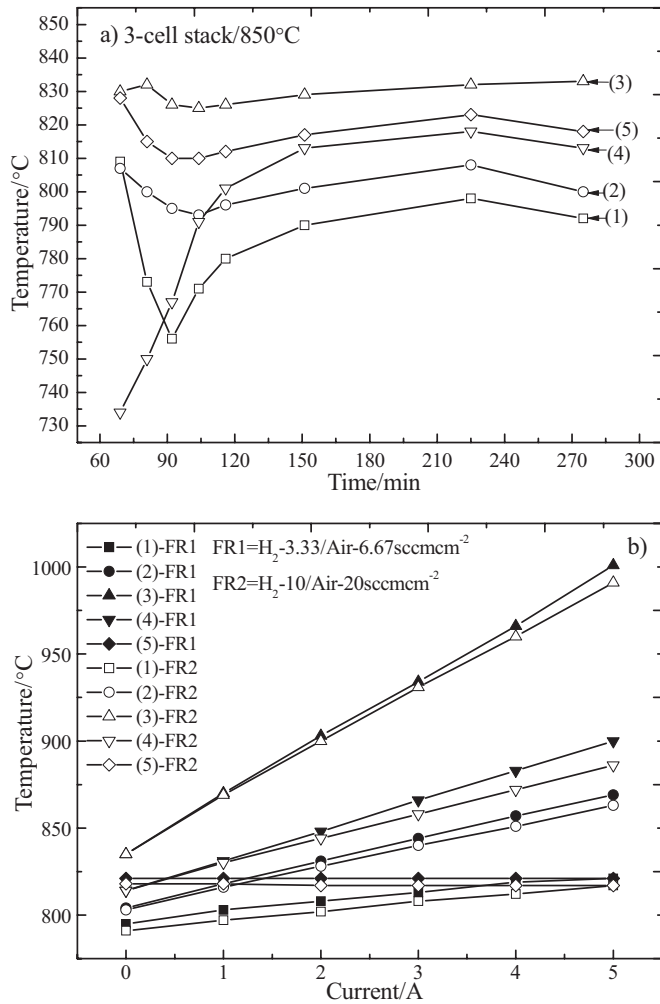
Fig. 8 The curve of temperatures with time course for various locations of the stack: (a) without discharging current; (b) the effect of discharging current on temperatures of various locations inside the stack with the flow rate of hydrogen/air of 3.33/6.67 sccm cm^{-2} and 10.00/20.00 sccm cm^{-2}. (1), (2), (3), (4), (5) indicating the position 1, 2, 3, 4, 5. FR1, FR2 indicating different gas flow rates.
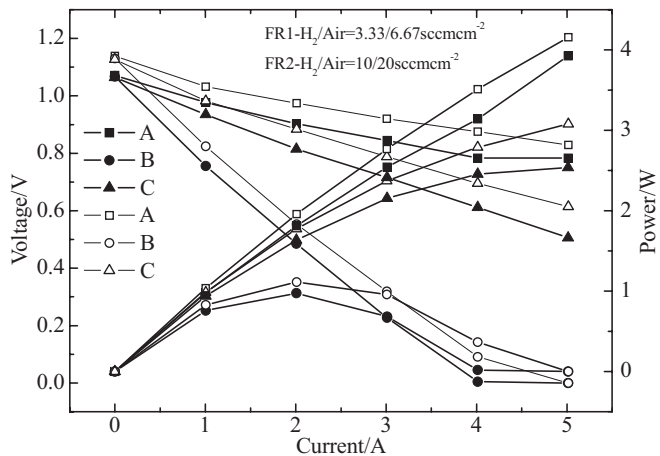

Fig. 9 I–V curves under different gas flow rate of the stack at the temperature of 850 °C, A, B, and C indicating Cell A, Cell B, and Cell C.
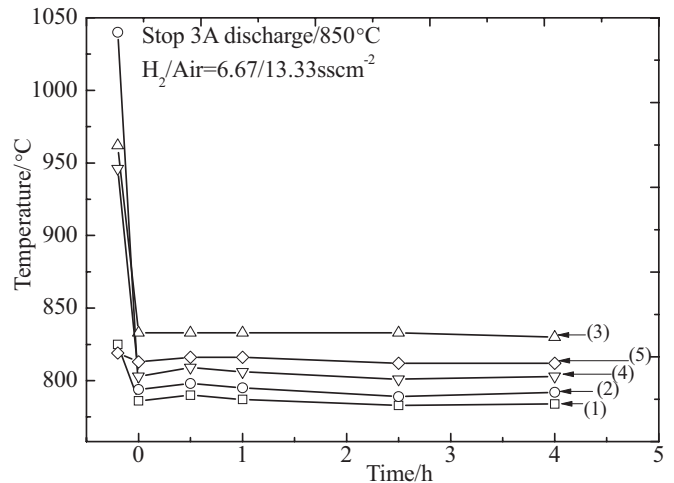

Fig. 10 Temperature changes with time course of various locations of the stack after a sudden stop of discharging current of 3 A.
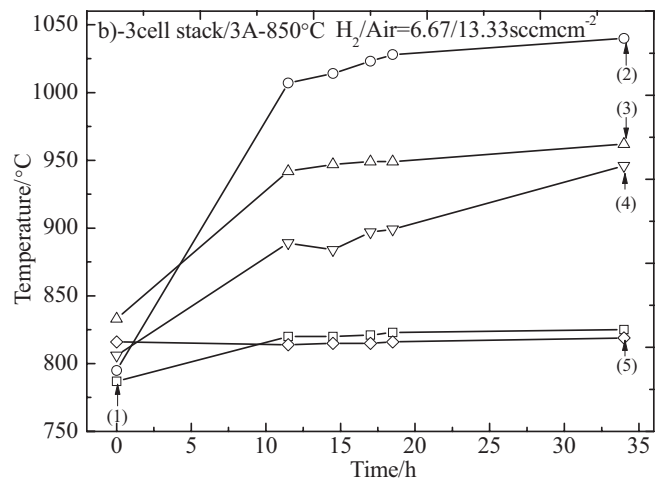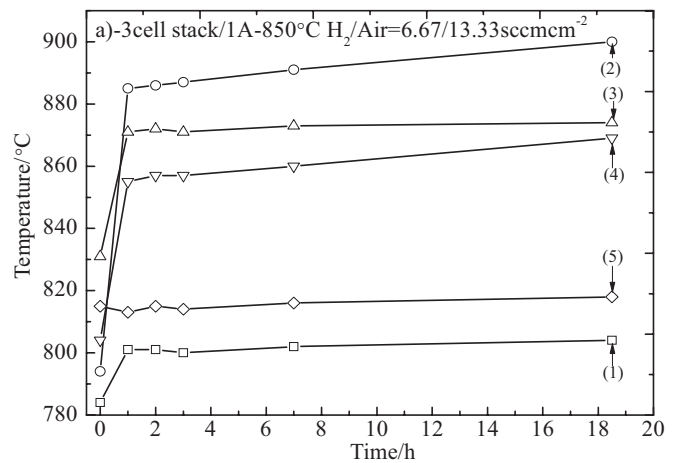

Fig. 11 The relation of discharging time vs. temperatures under various DC: (a) under 1 A, and (b) under 3 A.

curve of unit cell inside the stack. From the figure, it can be seen clearly the performance of unit cell is much low. Obviously, it can be concluded that the ohmic resistance of unit cell is much large. The increasing temperatures with the
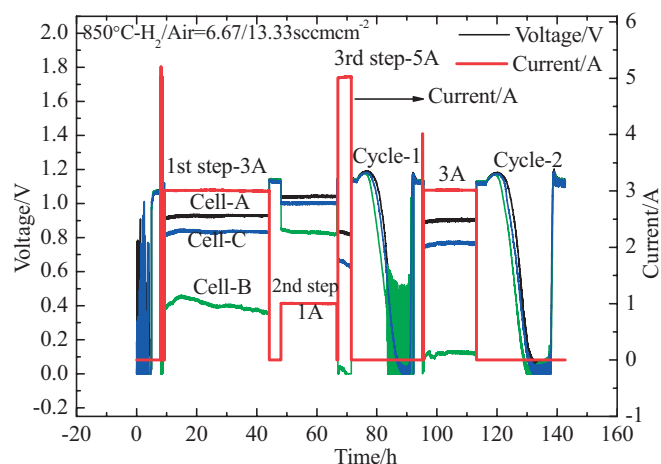
Fig. 12 The curve of OCV with time course under constant discharging currents, for voltage curve, form top to bottom, Cell A, Cell B, and Cell C.

increasing current are due to larger ohmic resistance with the current increases. Thus, the temperatures on cathode side inside the stack significantly increased with the increasing Joule heat resulting from the increasing current. Moreover, the increasing slopes of temperatures at various locations inside the stack are different because the resistances at various locations are different. To further verify the significant effect of discharging current on temperatures, a sudden stop of discharging current was carried out. Figure 10 showed the relationship between temperatures and time course after a sudden stop of discharging current. The results showed a rapid decline of the temperature at various locations and then remained stable, suggesting that current has a great impact on the cell surface temperature inside stack.

To investigate the relation of cell degradation under discharging *versus* temperature, the influence of discharging time on temperatures inside the stack under various constant DCs was investigated and the voltage changes of unit cells with time courses were carried out. Figure 11a and b showed that the temperatures at various locations on cathode side within stack increased rapidly, then increased slow and remained relatively stable under a constant discharging current of 1 and 3 A after a certain time, respectively. The temperature the location 5 (total hydrogen outlet) always almost remains unchanged during discharging at different current. The results indicated that the heat generated by current is mainly gathered in the cathode side. As seen from Figure 11, the first data point at the time of 0 is lower than the second data point (with discharging current), which the sudden increases in temperature on cathode side affected by current further indicating the great effect of discharging current on temperatures. In contrast to Figure 8a, after a short period of discharging, the order of the temperatures inside the stack changed obviously (seen in Figure 11), and the temperature at position 2 is higher than that of position 3, suggesting the temperature distribution on cell inside stack is much non-uniform. Figure 12 represents the voltage–time (V–T) curves under constant current discharging. At the first step before

thermal cycling, the stack was discharged at 3 A DC. The corresponding voltage of cell A and cell C almost remains stable, while the voltage of cell B decreased apparently. At the second step before thermal cycling, the discharged current of the stack is decreased to 1 A. Also, it can be seen that the corresponding voltage of cell A and cell C keeps stable and the voltage of cell B decreased. It also can be seen that the voltage decline of cell B at 1 A constant discharging is significantly less than that at 3 A constant discharging. The effect of discharged current on cell temperature was reviewed, as seen in Figure 11. It can be found that under the constant current of 3 A, the temperatures of cell B (position 2 and 3) increase more sharply than those under the constant current of 1 A, corresponding to a significant voltage decline of cell B. The temperature of cell A and C at air inlet and air outlet under 1 A and 3 A discharging current is all lower than that of cell B and all below the temperature of 950 °C. Correspondingly, the voltage of cell A and cell B is much higher and more stable than that of cell B. The results of relationship between temperature and discharging time under a constant current obtained in this work by experimental methods is consistent with those obtained by using numerical simulation method [13], in which the temperatures of unit cell with high performance were less than that of cell with low performance inside the stack for anode-supported SOFCs. From the above observation, it can be summarized that, under a constant current, the decay of unit cell will cause the voltage drop, and further cause increasing the temperature of cell surfaces. Two thermal cycling experiments were then carried out for the three-cell stack. The OCV of unit cell inside the stack always remains more than 1.1 V, indicating that the inserted thin thermocouple into the stack from the middle of the multi-layer sealant had little effect on stack sealing performance. The results also showed that the thin K-type thermocouple can be used for measuring temperature inside stack.

4 Conclusions

An experimental method to measure temperatures of unit cells inside SOFC stacks was developed by using thin K-type thermocouples and self-developed CAS-I sealing materials, in which the thin K-type thermocouple is inserted into the stack from the middle of the multi-layer sealant. The sealant was proven to have a good sealing effect by characterization and experiment. Using this method, the temperature of unit cells inside stacks was measured and investigated. The results showed the discharging DC has a significant impact and the gas flow rate has a slight impact on the temperatures inside SOFC stacks. Moreover, the temperature distribution inside the stack is much non-uniform. The air inlet temperature is lower than that of the air outlet at the initial discharging and the maximum temperature difference between outlet and inlet is close to 200 °C with a constant air rate of 20 sccmcm^{-2}. However, for decaying unit cells, the air inlet temperature is higher than that of air outlet after a short peri-

od of discharging. Moreover, the appearance of high temperatures is a sign of the cell decay (voltage drop), suggesting the importance of minimizing the temperature gradients.

Acknowledgements

References

[1] P. Leone, A. Lanzini, P. Squillari, P. Asinari, M. Santarelli, R. Borchiellini, M. Calì, *International Journal of Hydrogen Energy* **2008**, *33*, 3167.

[2] M. Iwata, T. Hikosaka, M. Morita, T. Iwanari, K. Ito, K. Ond, Y. Esaki, Y. Sakaki, S. Nagata, *Solid State Ionics* **2000**, *132*, 297.

[3] C. M. Dikwal, W. Bujalski, K. Kendall, *Journal of Power Sources* **2009**, *193*, 241.

[4] J. Malzbender, R. W. Steinbrech, *Journal of Power Sources* **2007**, *173*, 60.

[5] M. Pihlatie, A. Kaiser, M. Mogensen, *Journal of the European Ceramic Society* **2009**, *29*, 1657.

[6] C. K. Lin, T. T. Chen, Y. P. Chyou, L. K. Chiang, *Journal of Power Sources* **2007**, *164*, 238.

[7] L. K. Chiang, H. C. Liu, Y. H. Shiu, C. H. Lee, R. Y. Lee, *Renewable Energy* **2008**, *33*, 258.

[8] M. Lockett, M. J. H. Simmons, K. Kendall, *Journal of Power Sources* **2004**, *131*, 243.

[9] A. A. Kulikovsky, *International Journal of Hydrogen Energy* **2010**, *35*, 308.

[10] T. L. Wen, D. Wang, H. Y. Tu, M. Chen, Z. Lu, Z. Zhang, H. Nie, W. Huang, *Solid State Ionics* **2002**, *152–153*, 399.

[11] H. Y. Jung, S. H. Choi, H. Kim, J. W. Son, J. Kim, H. W. Lee, J. H. Lee, *Journal of Power Sources* **2006**, *159*, 478.

[12] T. S. Li, H. Miao, T. Chen, W. G. Wang, C. Xu, *Journal of the Electrochemical Society* **2009**, *156*, B1383.

[13] A. C. Burt, I. B. Celik, R. S. Gemmen, A. V. Smirnov, *Journal of Power Sources* **2004**, *126*, 76.

—————————————————————